한국음향학회지 제33권 제5호 pp. 282~290 (2014)
The Journal of the Acoustical Society of Korea Vol.33, No.5 (2014)
http://dx.doi.org/10.7776/ASK.2014.33.5.282

pISSN : 1225-4428
eISSN : 2287-3775

Numerical Analysis of the Backscattering Amplitude for a Partially Buried Cylinder on a Flat Interface Using Method of Moments

모멘트법을 이용한 경계면에 부분적으로 파묻힌 실린더의 음향 후방산란에 대한 수치해석

Kyungmin Baik† and Philip L. Marston*

(백경민,† Philip L. Marston*)

Center for Fluid Flow and Acoustics, Korea Research Institute of Standards and Science, University of Science and Technology
*Department of Physics, Washington State University, U.S.A.

(Received March 12, 2014; accepted July 11, 2014)

ABSTRACT: Though there have been advances in the numerical analysis of the acoustic scattering by smooth objects, numerical analysis of the acoustic scattering by the objects that are partially exposed on the interface are still rare. In determining the backscattering amplitude by a partially buried cylinder on a seabed, reverberation by the interface changes the feature of the scattering form function. Current study adopted the Method of moments (MoM) to provide the numerical analysis on the backscattering amplitude for a partially buried cylinder on a flat interface. Suggested numerical analysis showed the good agreements with the measurements and the analytic solution obtained by the Kirchhoff approximation. Numerical analysis described in the current study can be applied to the backscattering problem of any shape of the objects partially imbedded on a seabed by combining the reverberation from the seabed with the scattered wave from the objects.
Keywords: Backscattering, Buried cylinder, Seabed, Method of moments
PACS numbers: 43.30.Gv, 43.20.EI, 43.20.Fn.

초 록: 매끈한 물체에 의한 음향산란에 관한 수치해석은 발전해 왔으나 경계면에 위로 부분적으로 드러나 있는 물체에 의한 음향산란에 대한 수치해석은 여전히 드물다. 해저면에 부분적으로 파묻힌 실린더의 후방산란진폭을 결정함에 있어 경계면에 의한 잔향은 표적의 산란 함수 특성을 변화시킨다. 본 연구는 평탄한 경계면에 부분적으로 파묻힌 실린더의 후방산란진폭에 대한 수치해석을 제시하기 위하여 모멘트법(Method of Moments)을 채택하였다. 제시된 수치해석은 측정 및 키르히호프 근사법으로 얻은 해석적인 해와 상당한 일치를 보여주었다. 본 연구에서 기술된 수치해석은 해저면에서의 잔향과 표적으로부터의 산란파를 결합시킴으로써 해저면에 부분적으로 파묻힌 어떠한 형상의 표적에 대한 후방산란 문제에도 적용될 수 있다.
핵심용어: 후방산란, 파묻힌 실린더, 해저면, 모멘트법

I. Introduction

Although the investigation of the scattering of sound by partially buried object in sediment has been performed experimentally,[1] and theoretically,[2] the development of *fast* numerical methods could be helpful for giving insight into aspects of the scattering for a partially buried object. Method of Mements (MoM) is a kind of numerical technique assuming the object is composed of small segments which has a step-function like impulse response.[3] MoM is a fast and accurate numerical approach especially in the scattering

†**Corresponding author:** Kyungmin Baik (kbaik@kriss.re.kr)
Center for Fluid Flow and Acoustics, Korea Research Institute of Standards and Science, 267 Gajeong-Ro, Yuseong-Gu, Daejeon 305-340, Republic of Korea
(Tel: 82-42-868-5208, Fax: 82-42-868-5643)
"이 논문은 2013년 한국음향학회 추계학술발표대회에서 발표하였던 논문입니다."

problem for a complete smooth object. However, when the object is suddenly trucated by the interface, implementation of the MoM technique for the scattering problem is questioned. This work examines the application and the testing of the MoM to a simple case when the sound is incident and is backscattered from the 2D rigid cylinder truncated by a soft or rigid flat interface. In such case, backscattering amplitude from the cylinder is greatly affected by the reverberation from the interface.[4] In the current study, MoM technique is applied by combing the scattering from the object with the reverberation from the interface.

II. MoM Technique for a 2D cylinder in free-field

Generally, the acoustically scattered pressure by a two dimensional smooth cylinder is given as follow in the $\exp(+j\omega t)$ convention:[5]

$$P_s(\vec{x}) = \frac{1}{4j}\int_A s(\vec{x}')H_0^{(2)}\{k|\vec{x}-\vec{x}'|\}dA_{x'}, \quad (1)$$

where $P_s(\vec{x})$ is the scattered pressure, $s(\vec{x}')$ is the kernel, and $H_0^{(2)}$ is a zeroth-order Hankel function of the second kind. Vector $\vec{x}$ represents the observed direction, $\vec{x}'$ means the integrated segments location, and $dA_{x'}$ is the area of the cylinder that the segments are integrated. The basic concepts of the MoM is approximating the kernel $s(\vec{x}')$ by using the propagator $H_0^{(2)}$ and the incident pressure P_i. Once the kernel $s(\vec{x}')$ is obtained, the scattered pressure $P_s(\vec{x})$ can be calculated from Eq.(1). At the surface of the cylinder, rigid acoustical boundary condition is imposed, which is $\partial P_{\text{total}}/\partial n = 0$. Because $P_{\text{total}} = P_i + P_s$, on the surface of the rigid cylinder with the radius of a, the following relationship is satisfied:

$$\left.\frac{\partial P_i(\vec{x})}{\partial n}\right|_{|\vec{x}|=a} = -\left.\frac{\partial P_s(\vec{x})}{\partial n}\right|_{|\vec{x}|=a}. \quad (2)$$

Thus, substituting Eq.(1) into the r. h. s. of Eq.(2),

$$\left.\frac{\partial P_i}{\partial n}\right|_A = -\frac{1}{4ja}\int_A s'(\vec{x}')\left.\frac{\partial H_0^{(2)}(kR)}{\partial n}\right|_A dA_{x'}, \quad (3)$$

where the subscript A represents the surface of the cylinder and $R=|\vec{x}-\vec{x}'|$. For a convenience, the kernel $s'(\vec{x}') = as(\vec{x}')$ was introduced here where a is cylinder radius. Gradient of the Hankel function with respect to the coordinates $\vec{x}$ is obtained as:

$$\nabla H_0^{(2)} = -\frac{k}{R}\{(x-x')\hat{x}+(y-y')\hat{y}\}H_1^{(2)}(kR). \quad (4)$$

When the observation point is arbitrary location on the surface of the cylinder as shown in the geometry of Fig. 1, $x-x'$, $y-y'$, R, and the normal vector on the surface, $\hat{n}$, are calculated as:

$$x - x' = a(\cos\theta - \cos\theta'), \quad (5a)$$

$$y - y' = a(\sin\theta - \sin\theta'), \quad (5b)$$

$$R = 2a\left|\sin\left(\frac{\theta-\theta'}{2}\right)\right|, \quad (5c)$$

$$\hat{n} = \hat{x}\cos\theta + \hat{y}\sin\theta. \quad (5d)$$

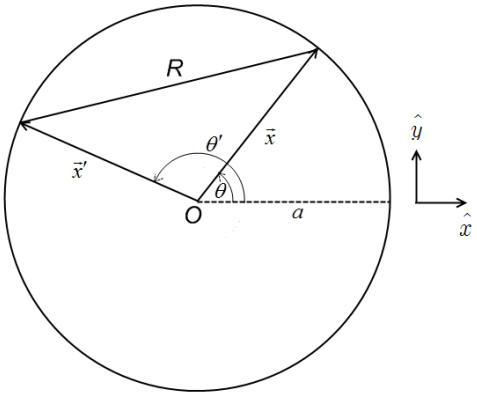

Fig. 1. Geometry of the cylinder. R is the distance between vectors $\vec{x}$ and $\vec{x}'$, and a is cylinder radius.

Then, normal derivative of Hankel function with respect to the coordinates $\vec{x}$ becomes:

$$\frac{\partial}{\partial n}H_0^{(2)}(kR) = -k\left|\sin\left(\frac{\theta-\theta'}{2}\right)\right|H_1^{(2)}(kR), \tag{6}$$

thus, Eq.(3) is expressed as:

$$\left.\frac{\partial P_i}{\partial n}\right|_A = \frac{k}{4ja}\int s'(\vec{x}')\left|\sin\left(\frac{\theta-\theta'}{2}\right)\right| \times H_1^{(2)}(kR)dA_{x'}. \tag{7}$$

Introducing the kernel $s'(\vec{x}')$ as a superposition of the unit-step basis functions such as:

$$s'(\vec{x}') = \sum_{n=1}^{N} a_n P_n(\vec{x}'), \tag{8a}$$

$$P_n(\vec{x}') = \begin{cases} 1, & \vec{x}' \in n^{th}\ \text{cell} \\ 0, & \text{otherwise} \end{cases}. \tag{8b}$$

then, for a given incident pressure at *m*-th cell, Eq.(7) is discretized as:

$$\left.\frac{\partial P_i}{\partial n}\right|_{m^{\text{th}}} = \frac{k}{4j}\sum_{n=1}^{N} a_n \times \int_{n^{\text{th}}}\left|\sin\left(\frac{\theta-\theta'}{2}\right)\right|H_1^{(2)}(kR)d\theta'. \tag{9}$$

Eq.(9) tells that a given incident pressure at *m*-th cell can be expressed as the product of unknown coefficient a_n and the integration of $|\sin[(\theta-\theta')/2]|H_1^{(2)}(kR)$ within *n*-th cell, which is displayed as an element of the impedance matrix in Eq.(11). Therefore, for the *N*-numbers of cases from $m=1$ to $m=N$, Eq.(9) constitutes following matrx equation

$$\mathbf{INC} = \mathbf{Z}\boldsymbol{a_n}, \tag{10}$$

where INC is $N\times 1$ incident matrix, Z is $N\times N$ impedance matrix, and $\boldsymbol{a_n}$ is $N\times 1$ unknown coefficients describing the kernel $s(\vec{x}')$. When the kernel $s'(\vec{x}')$ is discretized on the surface of the cylinder, in order to give accurate results on the scattering form function, $d\theta'$ should satisfy the condition of $d\theta' \le \pi/(ka)$ where ka is wavenumber-radius product in propagating medium. Such condition can be derived by the Nyquist sampling theorem.

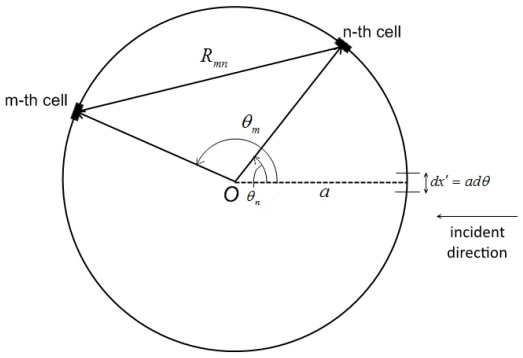

Fig. 2. Geometry of the MoM elements on the cylinder. Indices for the observed cell and the local cell are denoted as m and n respectively.

Fig. 2 shows the geometry to calculate the matrix elements of INC and Z. Locations of the centers of the *m*-th cell and the *n*-th cell are denoted as θ_m and θ_n respectively. Distance between centers of *m*-th cell and *n*-th cell is denoted as R_{mn}. At the location of *m*-th cell, normal derivative of the incident pressure can be approximated as the value at the center of *m*-th cell if size of the cell is sufficiently small compared to the wavelength of the incident pressure. Thus, for the *m*-th cell, normal derivative of the incident pressure becomes:

$$\left.\frac{\partial P_i}{\partial n}\right|_{m^{\text{th}}} = jke^{jka\cos\theta_m}\cos\theta_m, \tag{11}$$

where incident direction is along -$\hat{x}$ as shown in Fig. 2. Calculation of the elements of the impedance matrix Z_{mn} are different for the off-diagonal elements where $m \neq n$ and diagonal elements where $m = n$. The result of the calculation of impedance matrix which is independent of the incident direction is as follows:[3]

$$Z_{mn} \approx \begin{cases} -\frac{1}{2a}, & (m=n) \\ -\frac{k\Delta\theta}{4j}\left|\sin\left(\frac{\theta_m-\theta_n}{2}\right)\right| \\ \times H_1^{(2)}(kR_{mn}), & (m\neq n) \end{cases} \quad (12)$$

Once matrix a_n is obtained by $a_n = Z^{-1}INC$, the scattered pressure can be evaluated by substituting the kernel $s'(\vec{x}')$ with the matrix a_n in Eq.(1). For the far-field scattering, far-field pressure can be approximated by using following approximation for the Hankel function at large argument:[6]

$$H_0^{(2)}(kR) \approx \sqrt{\frac{2j}{\pi k\rho}}e^{-jkR}. \quad (13)$$

Because distance R from the point scattered to the observed point can be approximated as $R \simeq \rho-(x\cos\phi + y\sin\phi)$ at the far-field as shown in Fig. 3 where angle ϕ is direction of the observed point, the resulting scattered pressure can be expressed as

$$P_s(\vec{x}) = e^{-jk\rho}\frac{1}{4j}\sqrt{\frac{2j}{\pi k\rho}}\Delta\theta \times\sum_{n=1}^{N} a_n e^{jk(x_n\cos\phi+y_n\sin\phi)}. \quad (14)$$

Hence, using the above expression, calculating the scattering amplitude f,

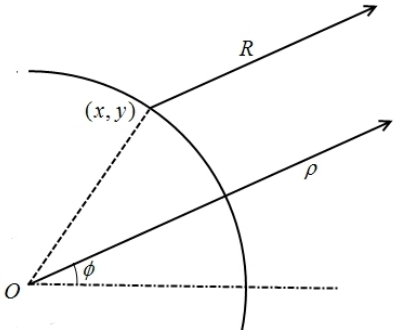

Fig. 3. Geometry of the far field approximation. When a source is assumed to be located in the infinity, the direction vector from the center of the cylinder and the vector from the cell are parallel to each other.

$$|f| = \frac{\Delta\theta}{2\sqrt{\pi k}}\left|\sum_{n=1}^{N} a_n e^{jz\cos(\theta_n-\phi)}\right|, \quad (15)$$

and normalizing $|f|$ with respect to $\sqrt{a/2}$, the dimensionless form function $|f|_{\mathrm{norm}}$ is obtained as

$$|f|_{\mathrm{norm}} = \frac{\Delta\theta}{2\sqrt{\pi z}}\left|\sum_{n=1}^{N} a_n e^{jz\cos(\theta_n-\phi)}\right|, \quad (16)$$

where $z=ka$ is wavenumber radius product. In Eq.(16), the direction of the far-field is determined by the angle ϕ and the incident pressure determines the value of a_n from Eq.(10). In case of the backscattering, the incident angle is identical to the angle ϕ.

The exact solution of the scattering amplitude of a 2D cylinder for the broad side incidence is well known as follows in $\exp(-i\omega t)$ convention:[7]

$$f_{\mathrm{norm}} = -\frac{2}{\sqrt{\pi z}}e^{-i\pi/4}\sum_{m=-\infty}^{\infty} e^{im\phi}\frac{J_m'(ka)}{H_m^{(1)'}(ka)}. \quad (17)$$

Fig. 4 shows the comparison of the MoM results in Eq.(16) with the exact solution in Eq.(17) for four different values of $z=ka$ as a function of the scattering direction, ϕ. Black dots represent the result of MoM simulation and the solid lines are the exact solution. ka values range from 5 to 20. All MoM simulations were done using 1000 number of equal line segments along the circumference of the cylinder, which satisfies the condition of $\Delta\theta \le \pi/(ka)$. In evaluating Eq.(17), the infinite series of Bessel function or Hankel function were substituted as the finite series with the proper choice of the truncation which is the maximum value of index m. The truncation limit $M=m_{\max}$ was chosen as $M=10+2ka+9.1(ka)^{1/3}$ which is the sufficient value that does not affect the shape of the graph.[8] Around the scattering angle of $\phi=0^\circ$, maximum peaks are observed, which is the effect of the forward scattering by the incident pressure. MoM results are consistent with the exact solution, however, at higher value of $ka=20$, the result is not accurate. Some abnormal

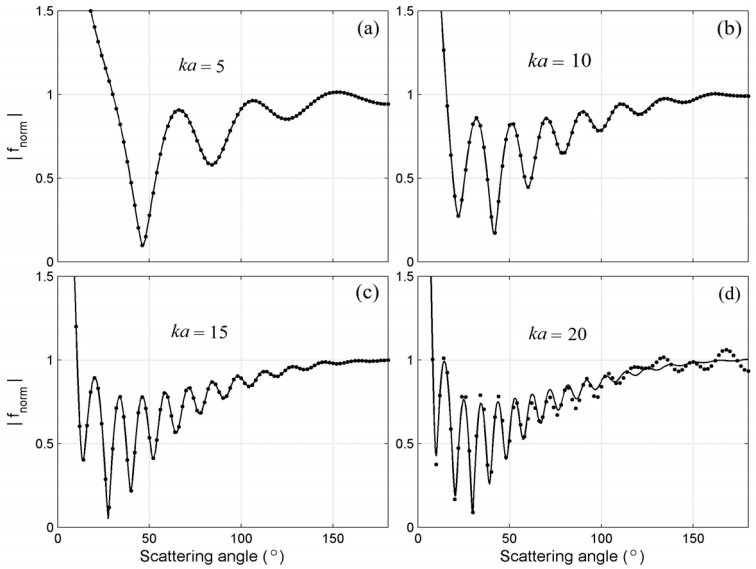

Fig. 4. Comparison of the exact solution with the MoM simulation for the scattering of the single infinite cylinder. Solid lines show the exact solution calculated from Eq. (17) and the black dots are MoM simulation with 360 elements. Comparison is done for the different values of ka such as (a) $ka=5$, (b) $ka=10$, (c) $ka=15$, and (d) $ka=20$. MoM shows the overall good agreements with the exact solution. But, at the special value of $ka=20$, it deviates severely from the expectation.

behavior of the MoM simulation happens at special values of ka. Such deviation between MoM results and exact solution comes from the numerical accuracy of the Bessel function implemented in MATLAB. Evaluation of Bessel function is critical to obtain impedance matrix as shown in Eq.(12). Over most values of *ka*, expression in Eq.(12) is enough to give accurate results on the scattering amplitude. However, for a certain value of *ka*, evaluation of Bessel function in MATLAB is not as accurate as other programs. When the same MoM calculation is performed for *ka*=20 with older version of MATLAB, errors between MoM results and the exact solution become much larger than Fig. 4(d) although such comparison was not shown in the current study. It is not also shown here that when more accurate expression of impedance matrix was adopted, the errors between MoM results and the exact solution was suppressed.

III. MoM Technique for a 2D cylinder partially buried on a flat interface

When considering the scattering for a buried object on a flat interface, two incident pressure are considered as shown in Fig. 5 which shows the partially buried cylinder and its image cylinder. Grazing angle is denoted as θ_i. At a given point B on the surface of the cylinder, two pressures contributes its total incident pressure. One is the directly incident pressure from the plane wave source and the other is the reflected pressure from the flat interface. In the current study, two kinds of flat interfaces are considered: soft interface where total pressure vanishes and the rigid interface where the normal derivatives of the total pressure vanishes, which modifies the phase of the reflected pressure from the flat interface.

From Fig. 5, incident pressure P_{in} onto the point B, in $+j\omega t$ convention, is expressed as $P_{\text{in}}=\exp[jka\cos(\theta-\theta_i)]$. Path difference between P_{in} and P_{ref} is the same as the length $\overline{B'C}=\overline{BB'}\sin\theta_i$. Length $\overline{BB'}$ is the same as $2(h-a+a\sin\theta)$. So, the reflected pressure $P_{\text{ref}}=\pm P_{\text{in}}\exp(-jk\delta)$, where $\delta=\overline{BB'}\sin\theta_i=2(h-a+a\sin\theta)\sin\theta_i$ and the positive and negative signs in front of P_{in} come from the rigid and soft boundary conditions of the interface respectively. Therefore the total

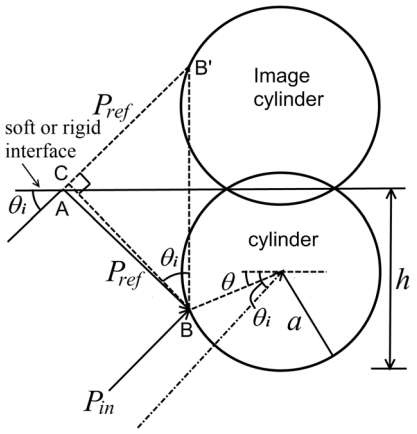

Fig. 5. Partially buried cylinder and its image cylinder. Grazing angle is denoted as θ_i. At a given point B on the surface of the cylinder, two pressure contributes its incident pressure. One is directly incident pressure from the source and the other is reflected pressure by the flat interface. Hence, total incident pressure is the sum of the directly incident pressure and the reflected pressure with the phase consideration. For the backscattering, the scattered pressure is the exact opposite process of the incident case.

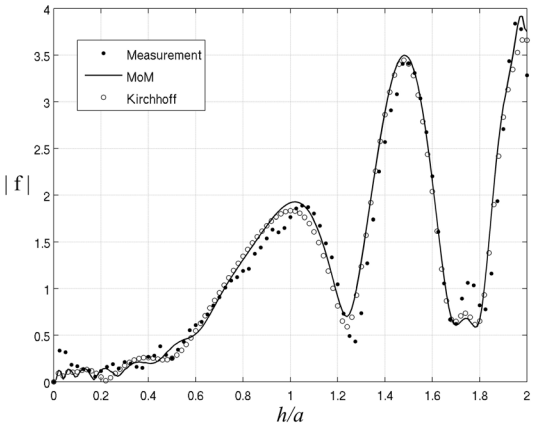

Fig. 6. Comparison of the experimental measurements with the analytic solution by the Kirchhoff approximation and the MoM simulation with 360 elements using Eqs. (19) and (20). Measurements are points, the Kirchhoff approximation are represented as blank circles, and the MoM results are plotted as solid line. Measurement is taken at 160 kHz. MoM results show similar features as the Kirchhoff approximation, but more oscillatory at the shallow depth of h less than $0.4a$.

pressure onto the point B becomes

$$\begin{aligned} P_{\text{total}}^{\text{in}} &= P_{\text{in}} + P_{\text{ref}} \\ &= e^{jka\cos(\theta-\theta_i)} \pm e^{j\Delta} e^{jka\cos(\theta+\theta_i)}, \end{aligned} \tag{18}$$

where $\Delta = 2ka(1-h/a)\sin\theta_i$ and (+) for rigid interface and (-) for soft interface. Then the incident matrix INC is the normal derivative of the total incident pressure in Eq.(18). But, we need to specify which line segments of the cylinder is buried and is not exposed. Thus, the line segments of the buried elements of the INC are considered as zeros as follows.

$$\text{INC}_m \approx \begin{cases} jk[e^{jka\cos(\theta_m-\theta_i)}\cos(\theta_m-\theta_i) \\ \pm e^{j\Delta}e^{jka\cos(\theta+\theta_i)}\cos(\theta_m+\theta_i)], \\ (\text{exposed elements}). \\ 0, (\text{buried elements}). \end{cases} \tag{19}$$

When Eq.(19) is substituted into Eq.(10), matrix a_n is obtained for the case of the scattering by a partially buried cylinder on a flat interface. Once unknown coefficient, a_n, is obtained, backscattering form function is obtained just making the scattering process exactly opposite to the incident process. Thus, total backscattered pressure consists of the pressure backcattered from the surface of the original cylinder and the scattered pressure toward the interface which is followed by the reflection from the interface to the plane wave source. Therefore, from the same approximation and the processes in Eqs.(14) ~ (16), the dimensionless form function $|f|_{\text{norm}}$ for a partially buried cylinder on a flat interface is

$$\begin{aligned} |f|_{\text{norm}} &= \frac{\Delta\theta}{2}\sqrt{\frac{z}{\pi}}\left|\sum_{n=1}^{N} a_n[e^{jz\cos(\theta_n-\theta_i)}\right. \\ &\quad \left. \pm e^{j\Delta}e^{jka\cos(\theta_n+\theta_i)}\right|. \end{aligned} \tag{20}$$

Fig. 6 shows the comparison of the experimental measurements of the backscattering form function for a partially exposed cylinder on an air-water interface with the analytic solution by Kirchhoff approximation[2] and the MoM simulation with 360 elements using Eqs.(19) and (20). For the detail experimental setup and the measurements,

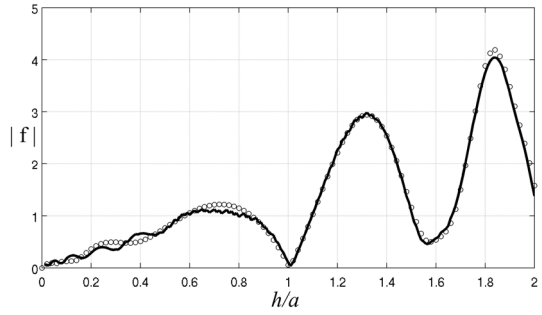

Fig. 7. Comparison of backscattering amplitude by the MoM simulation (solid) and the Kirchhoff approximation (blank circle) when the flat interface is rigid at the driving frequency of 140 kHz.

see Reference 2. Horizontal axis is the order of the exposure of the cylinder through the interface, which is normalized by a (see Fig. 5). The data were taken at 160 kHz with 30 degree grazing incidence ($\theta_i = 30°$) which are indicated as black dots. Because measurements were carried out for an air-water interface, soft boundary condition was used in the MoM simulation, thus, negative sign was adopted in Eqs.(19) and (20). MoM simulation is solid line and the analytic solution is denoted as blank circles. Both methods matches well with the measurem ents and show the same behavior with each other, however, at small *h*, MoM simulation is more oscillatory than the analytic solution.

Fig. 7 shows the Kirchhoff approximation and MoM simulation for the backscattering amplitude with rigid interface as a function of the *h* at 140 kHz. Solid lines represent the MoM simulation, and blank circles are the Kirchhoff approximation. Through all *h* of the cylinder, two methods show good agreements with each other. As shown in Fig. 6, MoM results are more oscillatory than the Kirchhoff approximation for small *h*.

As shown in Figs. 6 and 7, MoM simulation was performed for the partially submerged cylinder on a flat interface. Through the comparison of the MoM with the Kirchhoff approximation and measurements, we saw it was useful to describe a partially submerged cylinder. An exact solution can be calculated for the special case when the cylinder is halfway exposed, that is $h = a$. This problem

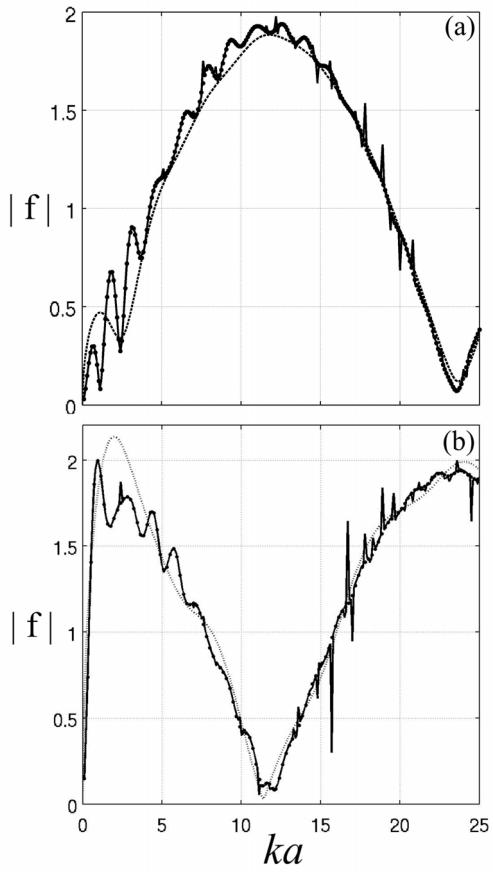

Fig. 8. Comparison of the exact solution (points) with the Kirchhoff approximation (dashed) and the MoM simulation (solid) for the half exposed rigid cylinder which has $h = a$ through (a) soft flat interface and (b) rigid flat interface. The horizontal axis is ka and vertical axis is the normalized backscattering amplitude. Incident angle of each picture is 30 degree. MoM results are much closer to the exact solution than the Kirchhoff approximation, however, at some value of the ka it returns the strange spikes.

was solved by Twersky[9] and derivation of the exact solution was shown in Reference 2. Figs. 8(a) and 8(b) show comparisons of the exact scattering amplitude with the Kirchhoff approximation and the MoM simulation with 360 elements as a function of ka from 0 to 25 at given incident angles of 30 degree when the cylinder is halfway exposed on a flat soft interface and on a flat rigid interface respectively. The measurements are denoted as black dots, the dashed line is Kirchhoff approximation, and the solid line represents MoM simulation. The exact solution shows more oscillatory behavior than the Kirchhoff approximation

and is very close to the MoM simulation. MoM results correspond to the exact solution regardless of low or high value of ka. But the strange spikes for certain ka values are seen. This is the same phenomena when the exact solution of the single cylinder scattering was compared with the MoM as shown in the Fig. 4. Sometimes the MoM returns severely deviated result which might be caused by the numerical convergence of the method. If such anomaly is fixed, MoM is more accurate method than Kirchhoff approximation regardless of rigid or soft boundaries of interface.

IV. Conclusions

The MoM simulation for the backscattering by a partially buried rigid cylinder on a soft or rigid flat boundary was presented. Comparing to the analytic solution calculated by the Kirchhoff approximation,[2] MoM technique for the problem shows the good agreements with the measurements and the exact solution as well as the Kirchhoff approximation. A key issue in the scattering by a partially buried object on a seabed is that the reverberation from the seabed greatly affects the scattering amplitude, which was shown analytically[2] in the previous study and numerically in the current study. Thus, the MoM technique presented in the currrent study can be applied to any shape of the smooth objects that are partially buried on a seabed if the reverberation from the seabed is known or well characterized.

Acknowledgement

This work was supported by the Office of Naval Research (ONR), USA.

References

1. A. Tesei, A. Maguer, W. L. J. Fox, R. Lim, and H. Schmidt, "Measurements and modeling of acoustic scattering from partially and completely buried, spherical shells," J. Acoust. Soc. Am. **112**, 1817-1830 (2002).
2. K. Baik and P. L. Marston, "Kirchhoff approximation for a cylinder breaking through a plane surface and the measured scattering," IEEE J. Ocean. Eng. **33**, 386-396 (2008).
3. A. F. Peterson, S. L. Ray, and R. Mittrar, *Computational Methods for Electromagnetics* (Wiley-IEEE press, New York, 1998), pp. 37-86.
4. J. W. Choi, K. S. Yoon, J. Na, J. S. Park, and Y. N. Na, "Shallow water high-frequency reverberation model" (in Korean), J. Acoust. Soc. Kr. **21**, 671-678 (2002).
5. D. S. Jones, *Acoustic and Electromagnetic Waves* (Oxford, New York, 1986), pp. 65-66.
6. M. Abramowitz and I. A. Stegun, *Handbook of Mathematical Functions with Formulas, Graphs, and Mathematical Tables*, 10th Ed. (Dover, Washington D.C. 1965), pp. 357-358.
7. A. L. Fetter and J. D. Walecka. *Theoretical Mechanics of Particles and Continua*, Dover Ed. (Dover, New York, 2003), pp. 337-338..
8. P. L. Marston, "Kirchhoff approximation for backscattering by partially illuminated circular cylinders: Two-dimensional case," J. Acoust. Soc. Am. **114**, 2302 (2003).
9. V. Twersky, "On scattering and reflection of sound by rough surfaces," J. Acoust. Soc. Am. **29**, 209-225 (1957).

Profile

▸ Kyungmin Baik(백경민)

He received the B. S. and M. S. degrees in physics from Korea University, Seoul, South Korea, in 1996 and 2000, respectively, and the Ph. D. degree in physics from Washington State university, Pullman, WA, USA, in 2008 under the supervision of Dr. Philip L. Marston. He carried out a research about bubble acoustics as a research fellow at the Institute of Sound and Vibration Research (ISVR), University of Southampton, UK, under the supervision of Dr. Timothy G. Leighton from 2008 to 2010. He conducted a research about underwater acoustics as a postdoctoral scholar at the Woods Hole Oceanographic institution (WHOI), MA, USA, under the supervision of Dr. Timothy K. Stanton from 2010 to 2012.
Currently, he is a senior researcher at the Korea Research Institute of Standards and Science (KRISS), Daejeon, South Korea since 2012. He is a member of the Acoustical Society of America.

▸ Philip L. Marston

He received the M. S. degrees in physics and electrical engineering and the Ph. D. degree in physics from Stanford University, Stanford, CA, in 1972, 1974, and 1976, respectively.

He was a Postdoctoral Fellow at Yale University, New haven, CT, from 1976 to 1978 and has been on the Faculty of Washington State University, Pullman, since 1978, where he is currently a Professor of Physics.

Dr. Marston was an Alfred P. Sloan Research Fellow from 1980 to 1984 and is a Fellow of the Acoustical Society of America.